 CMES, vol.114, no.2, pp.141-152, 2018

Automatic Delineation of Lung Parenchyma Based on Multilevel Thresholding and Gaussian Mixture Modelling

S. Gopalakrishnan[1, *] and A. Kandaswamy[2]

Abstract: Delineation of the lung parenchyma in the thoracic Computed Tomography (CT) is an important processing step for most of the pulmonary image analysis such as lung volume extraction, lung nodule detection and pulmonary vessel segmentation. An automatic method for accurate delineation of lung parenchyma in thoracic Computed Tomography images is presented in this paper. The proposed method involves a segmentation phase followed by a lung boundary correction technique. The tissues in the thoracic Computed Tomography can be represented by a number of Gaussians. We propose a histogram utilized Adaptive Multilevel Thresholding (AMT) for estimating the total number of Gaussians and their initial parameters. The parameters of Gaussian components are updated by Expectation Maximization (EM) algorithm. The segmented lung parenchyma from the Gaussian Mixture model (GMM) undergoes an Adaptive Morphological Filtering (AMF) to reduce the boundary errors. The proposed method has been tested on 70 diseased and 119 normal lung images from 28 cases obtained from Lung Image Database Consortium (LIDC). The performance of the proposed system has been validated.

Keywords: Lung parenchyma delineation, thoracic computed tomography, multilevel thresholding, Gaussian mixture model, Adaptive Morphological Filtering.

1 Introduction

In the recent years, thoracic Computed Tomography (CT) has become the standard for diagnosing several lung diseases such as lung nodules, pulmonary embolism, and interstitial lung diseases etc. An early detection of lung disease helps improve the survival rate of the patient [Midthun (2011)].

Computer aided analysis of medical images has drawn the attention of the image processing community for the past two decades. The segmentation of lung parenchyma with other lung tissues in the thoracic CT image reduces the complexity of the computer aided analysis applications such as lung nodule analysis, lung parenchyma density analysis, blood vessel analysis, air way analysis, lung mechanics analysis and so on. The increasing number of applications of thoracic CT analysis require a simple and efficient lung parenchyma delineation technique [Mansoor, Bagci, Xu et al. (2014)].

[1] Department of Biomedical Engineering, PSG College of Technology, Coimbatore, Tamil Nadu, India.
Email: sgk.bme@psgtech.ac.in.

[2] Department of Biomedical Engineering, PSG College of Technology, Coimbatore, Tamil Nadu, India.
Email: akswamy.bme@psgtech.ac.in.

* Corresponding author: S. Gopalakrishnan. Email: sgk.bme@psgtech.ac.in.

Many researchers have proposed various techniques for computer aided segmentation of lung parenchyma within the thoracic CT images. However these techniques are semi-automatic that they require human intervention for the segmentation process [Lin, Yan and Chen (2005)].

(a) Inclusion of airways

(b) Exclusion of pleural nodules and pulmonary vessels

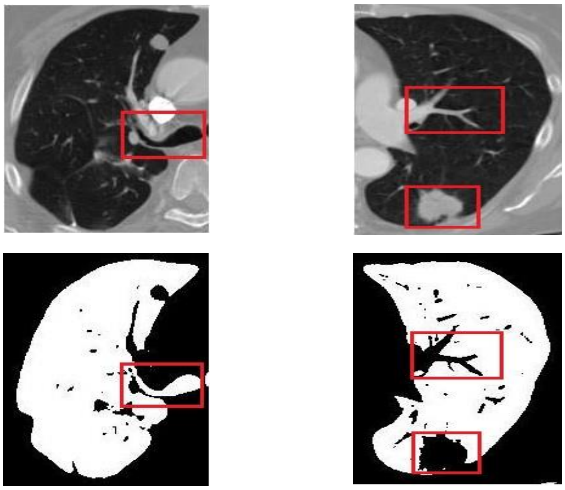

Figure 1: The limitations of gray level thresholding segmentation techniques

The limitations of thresholding based segmentation are depicted in Fig. 1. The Otsu's Adaptive Thresholding is used along with morphological opening and closing to segment the lung parenchyma [Yao, Bliton and Summers (2013)]. But such techniques are affected by severe edge distortions due to over smoothing of lung boundary which reduce the segmentation accuracy [Wei, Hu, MacGregor et al. (2008)].

In this work, we propose an unsupervised method for segmentation of lung parenchyma in a thoracic CT image. The proposed automatic delineation method consists of two phases: the segmentation stage and the lung border refinement stage as shown in Fig. 2. The first stage of lung parenchyma segmentation is based on Gaussian Mixture Model (GMM) which uses Expectation Maximization (EM) algorithm for updating the model parameters. The total number of Gaussian components and the initial parameters for each Gaussian component are obtained from Adaptive Multilevel Thresholding (AMT) technique which is proposed in this work. Finally, the lung border refinement is implemented using adaptive morphological filter. In order to validate the performance of the segmentation algorithm, the proposed method has been tested using Lung Image Database Consortium (LIDC) archive and the results are compared with other automatic segmentation techniques. The rest of the paper is organized as follows: Sections 2 and 3 describe the theoretical foundation for the proposed method and its performance metrics. Section 4 presents the experimental results of each stage of the segmentation algorithm. We conclude in Section 5 with a discussion for its potential clinical applications and its scope for future venture.

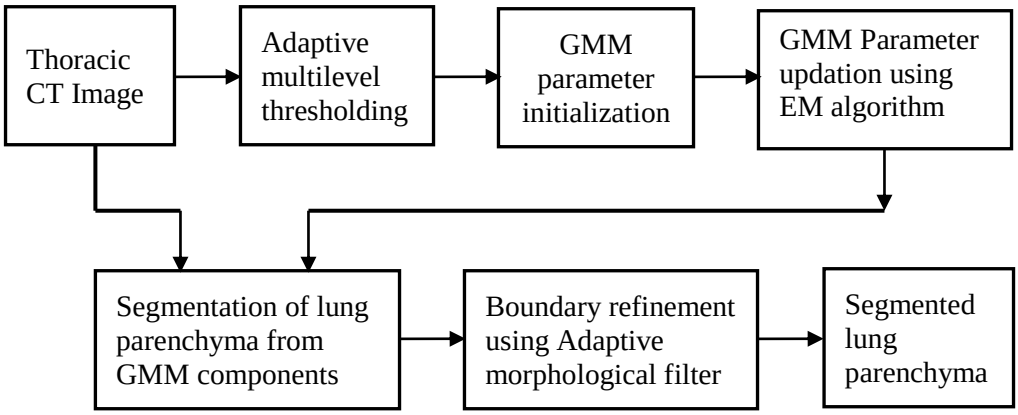

Figure 2: Block diagram of the automated lung parenchyma delineation technique

2 Lung parenchyma delineation

2.1 Initial parameter estimation

The initialization of the model parameters is an important processing step in the GMM segmentation frame work. Since EM algorithm is very sensitive about choice of the initial model parameters (μ_n, σ_n, π_n), an appropriate initial value of the model parameter will ensure the fast convergence of the algorithm to the best local maximum of the likelihood function. Sequential EM based initialization procedure has been proposed [Farag, El-Baz and Gimel'farb (2006)], which starts with a single Gaussian component covering the whole data set and it incrementally splits during expectation maximization steps. It may be repeated several times with different initial parameter values for giving the best approximation of the model. The other choices for initializing the model parameters are Fuzzy C-means [Sa (2010)] and K-means algorithm [Ji, Xia, Sun et al. (2012)].

2.1.1 Histogram analysis

The histogram of a digital image conveys some significant information about the different intensity regions. The intensity based image processing applications rely on the analysis of histogram [Gu, Kumar, Hall et al. (2013)]. The modes in the histogram represent an object or background and the gaps represent the degree of separation between the modes. The histogram of a typical lung CT is not flat, rather it has multiple modes and gaps and also these modes are not well separated. The overlapped modes in the histogram increase the complexity of the segmentation. The constituent part corresponding to different peaks of the histogram are shown in Fig. 3.

(a) Gray level histogram

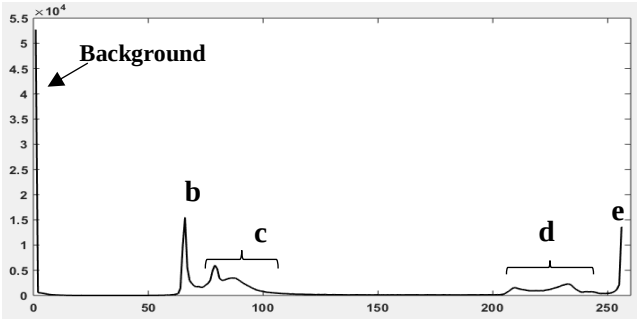

(b) Couch (c) Lungs (d) Soft tissues (e) Bones

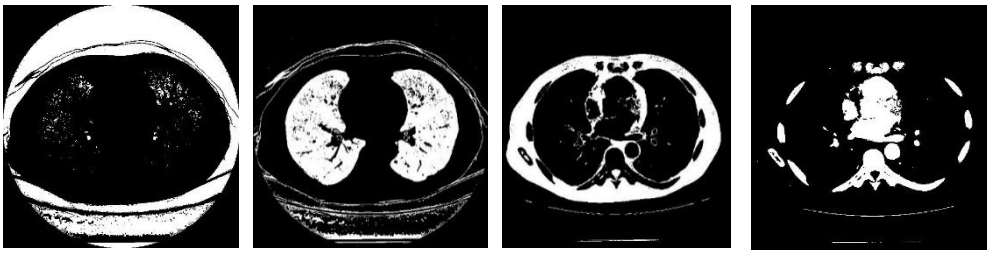

Figure 3: Histogram analysis of a typical lung CT image

2.1.2 Adaptive multilevel thresholding algorithm

The steps in adaptive multilevel thresholding algorithm are as follows:

Step 1: Obtain the Thoracic CT image, f

Step 2: Calculate the normalized histogram of the image, $P(r_k)$

Step 3: Find the first derivative of the Gaussian kernel, $\frac{\partial g(x,\sigma)}{\partial x}$

Step 4: Convolve the normalized histogram of the image with derivative of the Gaussian kernel, $C[n] = P(r_k) * \frac{\partial g(x,\sigma)}{\partial x}$

Step 5: Find the Zero crossings in $C[n]$ and calculate the number of peaks P_k and T_{k-1} intensity thresholds

Step 6: Apply multi-thresholding, $s = \begin{cases} L_1 \quad for \quad 0 \le f < T_1 \\ L_2 \quad for \quad T_2 \le f < T_3 \\ \vdots \\ L_k \quad for \quad T_k - 2 \le f < T_k - 1 \end{cases}$

Step 7: Obtain segmented image with k regions.

The steps involved in the multilevel thresholding process are illustrated in Fig. 4. There are four dominant modes excluding the first one which represents the background. The optimal separation of the modes is shown by a vertical dotted line.

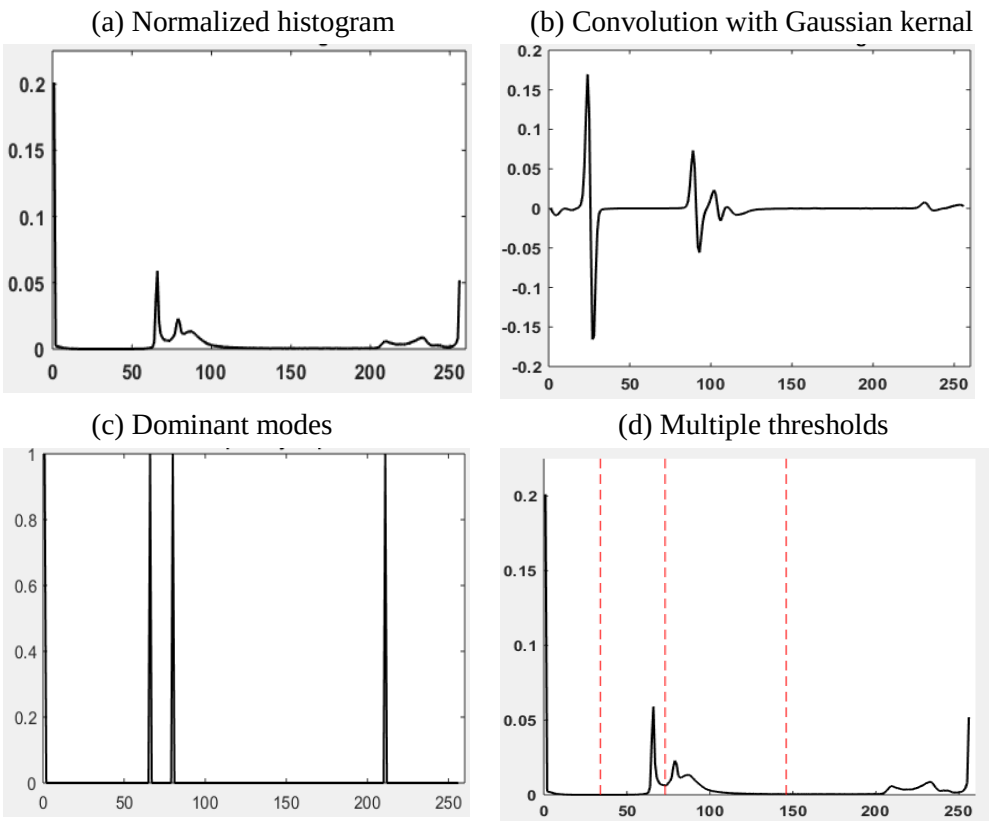

Figure 4: Adaptive multilevel thresholding

2.2 Gaussian mixture model based segmentation

Gaussian Mixture Model (GMM) is a generative model based on Bayesian theory and parameterized by mean and covariance. Its potential for complex image segmentation has been demonstrated by many researchers. GMM based multiple sclerosis lesion detection in brain MRI was proposed [Bijar and Khayati (2011)] using Active Contour Model (ACM) for parameter initialization. In this work, we attempt to speed up the convergence of the algorithm by introducing a simple method of estimating the initial model parameter and the number of Gaussian components.

Let G denote the set of gray intensities and N denote the total number of pixels in the thoracic CT image. Let K be the number of dominant peaks in the histogram of the image corresponding to K number of classes ($\omega_1, \omega_2, \ldots, \omega_K$). The observation of the i^{th} pixel is represented by x_i and this is assigned to a class with the largest posterior probability.

The Gaussian mixture model of the given observation x is

$$p(x) = \sum_{n=1}^{K} p(x|\omega_n) \quad (1)$$

Where ω_n is the parameter of the nth gaussian component, $\omega_n = (\mu_n, \sigma_n, \pi_n)$. The probability density function of the nth component is given by

$$p(x|\mu_n, \sigma_n) = \frac{1}{\sqrt{2\pi\sigma_n^2}} e^{\left(-\frac{\left((x_j - \mu_n)\right)^2}{2\sigma_n^2}\right)} \quad (2)$$

μ_n *and* σ_n are the mean and variance of the Gaussian distribution and π_n represents the mixture coefficient given by the prior probability of the corresponding class ω_n that independently generates all pixel labels y_n.

$$p(y_n = 1) = \pi_n \quad (3)$$

The mixture coefficients satisfy the following constraints

$$0 \leq \pi_n \leq 1 \quad (4)$$

$$\sum_{n=1}^{K} \pi_n = 1 \quad (5)$$

The log-likelihood of the density function given in (1) is

$$\ln p(x|\mu, \sigma, \pi) = \sum_{i=1}^{N} \ln \{\sum_{n=1}^{K} \pi_n \, p(x|\mu_n, \sigma_n)\}$$

Maximizing the log-likelihood function reduces the intra class variance of the model; therefore is better fit of the model and the data set can be achieved. Though the maximum likelihood (M-L) method provides a simple solution to GMM model, it fails when there are singularities in the data set and results in the log likelihood function getting into infinity [Allili, Bouguila and Ziou (2007)]. Another approach to estimate model parameter is gradient-descent optimization. Expectation Maximization (EM) has also been widely used to approximate the maximum likelihood [Greggio, Bernardino, Laschi et al. (2012); Nguyen, Wu, Member et al. (2010)]. The following two criteria play an important role in EM algorithm.

(i). The marginal distribution of *x*, which is obtained by summing the joint distribution *p(x|y)* over all possible states of *y* $p(x) = \sum_y p(y) \, p(x|y) = \sum_{n=1}^{K} \pi_n \, p(x|\mu_n, \sigma_n)$ (6)

(ii). The posterior probability $\psi(y_n)$, which can be obtained by using Bayes' rule in the conditional probability of y given x and using Eq. (6).

$$P(y_n = 1|x) = \psi(y_n) = \frac{P(y_n=1)P(x|y_n=1)}{\sum_{j=1}^{K} P(y_j=1)P(x|y_j=1)} = \frac{\pi_n \, p(x|\mu_n, \sigma_n)}{\sum_{j=1}^{K} \pi_j \, p(x|\mu_j, \sigma_j)} \quad (7)$$

2.2.1 Expectation maximization algorithm

EM algorithm is an iterative technique to determine the model parameters $\omega_n = (\mu_n, \sigma_n, \pi_n)$, ($n=1, 2, \ldots, K$). Each iteration has two steps, step of parameter estimation and step of parameter maximization. The step in estimation determines the posterior probability using the current parameter values and the step in maximization re-estimates the parameter using the posterior probabilities calculated in the former step. The expression used to update the parameters is obtained by differentiating the log-likelihood function with respect to the corresponding parameter μ_n *or* σ_n *or* π_n and setting it at zero. We obtain the following equations:

$$\mu_n^{(t+1)} = \frac{1}{N_n} \sum_{i=1}^{N} \psi(y_{in}) \, x_i \quad (8)$$

Where $N_n = \sum_{i=1}^{N} \psi(y_{in})$ represents the effective number of pixels assigned to the class n.

$$\sigma_n^{(t+1)} = \frac{1}{N_n}\sum_{i=1}^{N} \psi(y_{in})\,(x_i - \mu_n)(x_i - \mu_n)^{\mathrm{T}} \quad (9)$$

$$\pi_n^{(t+1)} = \frac{N_n}{N} \quad (10)$$

After training the GMM using Eq. (8-10), and determining $\psi(y_n)$ using Eq. (7), we can assign each pixel in the image to a class ω_n with largest $\psi(y_n)$.

2.3 Lung parenchyma boundary refinement

This section describes the morphological approach to the problem of lung boundary refinement. Lung parenchyma boundary correction based on top-hat transform has been proposed [Li-nan, Dao-jing, Shen-shen et al. (2010)], [Meng and Zhao (2009)], but these techniques use a constant size structuring element which results in a higher segmentation error. The technique proposed in our system is based on morphological filter that modifies the size of the structuring element based on local geometric features of the lung boundary. The mathematical morphological operations are represented by the combination of two basic operations: erosion and dilation. Let Z represent the set of integers and F (x, y) be a discrete image signal, where the set $\{x, y\} \subset Z^2$ is domain set and $\{F\} \subset Z$ is range set. The structuring element S can be expressed by its support domain $S \subset Z^2$. The erosion and dilation operation can be defined as

$$F \ominus S = \{Z|\ (S)_z \subseteq F\} \quad (11)$$

$$F \oplus S = \{Z|\ (\hat{S})_z \cap F \neq \emptyset\} \quad (12)$$

The opening and closing operations are defined as

$$(F \circ S)\,(x, y) = [(f \ominus S) \oplus S_1]\,(x, y) \quad (13)$$

$$(F \cdot S)\,(x, y) = [(f \oplus S) \ominus S]\,(x, y) \quad (14)$$

The opening operation removes objects that are smaller than the structuring element. Therefore, with a specified structuring element S_1, we can remove any small objects attached with the lung wall by taking the difference between the original image and the image processed by the opening operation which is described by the top-hat operation as follows,

$$\Upsilon\, S_1\,[F\,(x, y)] = \max\,[0, F\,(x, y) - (F \circ S_1)\,(x, y)] \quad (15)$$

Let S_2 be the second structuring element whose size should be larger than the lung mask used for background correction described by the operation

$$\Upsilon\, S_2\,[F\,(x, y)] = \max\,[0, F\,(x, y) - (F \circ S_2)\,(x, y)] \quad (16)$$

The desired enhanced image can be obtained by subtracting the results of the operation latter from that of the former.

3 Performance evaluation metrics

For evaluating the performance of the proposed system, we have imposed four metrics: Dice Similarity Coefficient (DSC), Sensitivity, Specificity and Hausdorff Distance (HD).

The total number of each combination of pixels for both manual and automatically labeled image is specified as follows:

- True Positive (TP) represents the total number of pixels which are correctly labeled by the algorithm.
- False Negative (FN) represents the number of lung parenchymal pixels the algorithm failed to label.
- False Positive (FP) represents the number of not a lung parenchymal pixel labeled as lung parenchyma by the segmentation algorithm.
- True Negative (TN) represents the number of pixels which are not labeled as lung parenchyma by both manual and automatic segmentation.

DSC is a statistical metric which quantifies the degree of likeness between the manual and automatic segmented images [Zou, Warfield, Bharatha et al. (2004)]. The Dice similarity coefficient is defined as

$$DSC = \frac{2TP}{2TP + FN + FP} \tag{17}$$

The DSC may take values between 0 and 1. If both the manual and automatic segmentation results are exactly identical then DSC will be equal to 1 and vice versa.

Sensitivity and specificity are statistical measures of the ability of the algorithm to correctly label the lung parenchymal pixels and correctly exclude not a lung parenchymal pixels respectively [Taha and Hanbury (2015)].

$$Sensitivity = \frac{TP}{TP + FN} \tag{18}$$

$$Specificity = \frac{TN}{TN + FP} \tag{19}$$

The Hausdorff distance provides a measurement of error between the two segmented regions [Chalana and Kim (1997)]. Let S_m and S_a be two surfaces, then the symmetrical Hausdorff distance is defined by,

$$d_h(S_m, S_a) = Max[d(S_m, S_a), d(S_a, S_m)] \tag{20}$$

Where

$$d(S_m, S_a) = \underset{p \in S_m}{Max} \; \mathrm{d}(p, S_a) \tag{21}$$

$$d(S_a, S_m) = \underset{p \in S_a}{Max} \; \mathrm{d}(p, S_m) \tag{22}$$

4 Data set and experimental results

The proposed method has been evaluated using the database created by lung image database consortium (LIDC) [Armato, McLennan, Bidaut et al. (2011)]. It is a large collection of publicly available referential thoracic CT database. We have covered 70 diseased and 119 normal lung images from 28 cases. The inclusion criteria entail the following features: should contain 40% of pathological lung image which includes pleural

nodules and 20% of the data contains airways and pulmonary vessels attached with lung walls. The ground truth images are carefully labeled with the help of experienced radiologists.

The results of the consecutive phases of the lung parenchyma segmentation process are shown in Fig. 5.

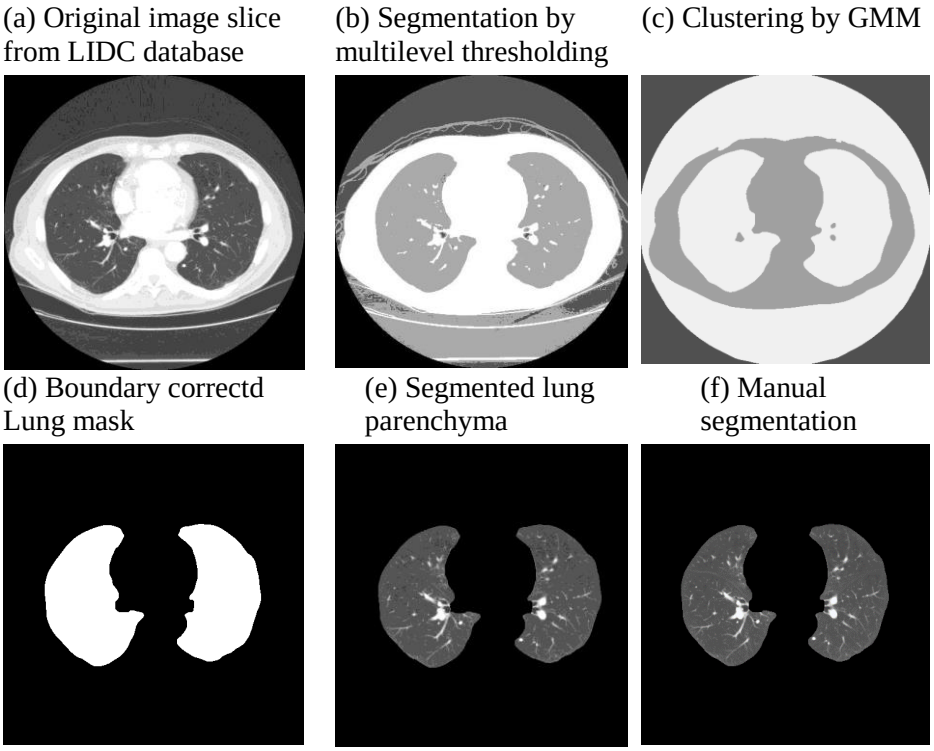

Figure 5: Result of the proposed method

The performance of the system achieved is evaluated in terms of its dice similarity coefficient (DSC), Hausdorff distance (HD), sensitivity and specificity values. The result of the proposed system and some of other segmentation algorithms reported in the literature such as fuzzy c-means clustering (FCM), combination of thresholding and rolling ball algorithm and GMM initialized by active contour segmentation (ACS) was computed and are summarized in Tab. 1.

Table 1: Performance of the lung segmentation algorithms

	DSC (%)	HD	Sensitivity (%)	Specificity (%)
Thresholding+Rolling ball	90.07	1.77	99.85	95.83
FCM+morphological filtering	93.74	1.44	99.76	97.52
ACS+GMM	96.03	1.18	99.49	99.35
Proposed	97.22	1.02	99.91	99.67

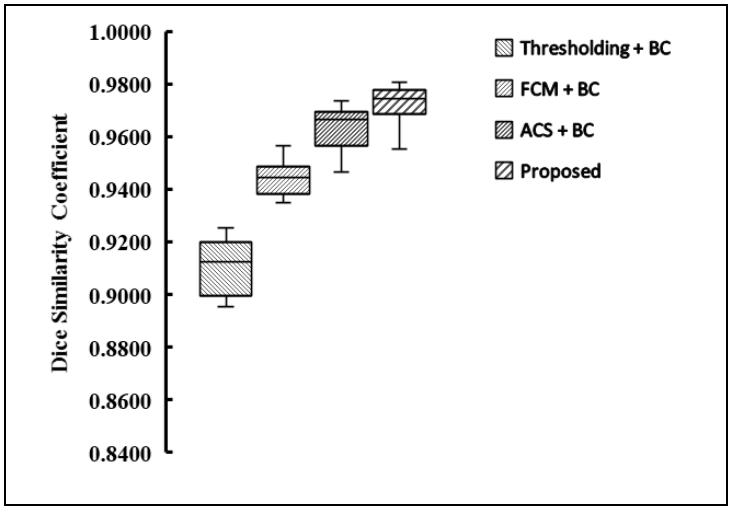

Figure 7: Comparison of the Dice similarity coefficient of the proposed and other automatic segmentation techniques

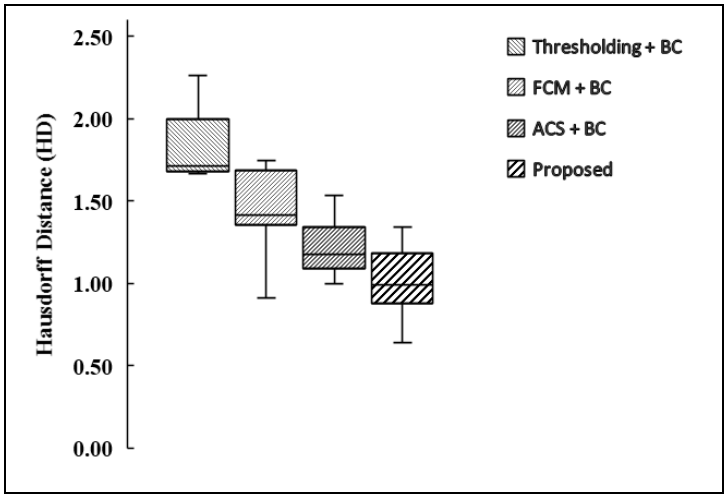

Figure 8: Comparison of the Hausdorff distance of the proposed and other automatic segmentation techniques

In order to evaluate the performance of the automatic segmentation algorithms, the segmentation results were compared with the ground truth produced by the radiologists. Based on Dice similarity coefficient and Hausdorff distance, the boxplots in Fig. 6 and Fig. 7 show the comparison among the automatic segmentation techniques.

5 Conclusion

In this paper we have presented an efficient lung parenchyma segmentation scheme for thoracic CT images. The scheme is fully automatic and does not require human

intervention. The proposed method involves GMM based segmentation followed by an adaptive border correction technique. This system provides a simple solution to the GMM initialization process which reduces the computational time. Furthermore, the adaptive boundary correction technique (that handle pathological lungs) improves the segmentation accuracy. These are the key features of the developed system. As demonstrated in this paper, it provides the highest segmentation accuracy (DSC=97. 22%) over other methods. Additionally, it also exhibits a very high sensitivity and specificity, which are significant in any computer aided diagnosis system. Hence the proposed lung parenchyma delineation scheme will be a promising precursor to the computer aided diagnosis of lung diseases.

References

Armato, S. G.; McLennan, G.; Bidaut, L.; McNitt Gray, M. F.; Meyer, C. R. et al. (2011): The lung image database consortium (LIDC) and image database resource initiative (IDRI): a completed reference database of lung nodules on CT scans. *Medical Physics*, vol. 38, no. 2, pp. 915-931.

Allili, M. S.; Bouguila, N.; Ziou, D. (2007): Finite generalized gaussian mixture Modeling and applications to image and video foreground segmentation. *Canadian Conference on Computer & Robot Vision*, vol. 17, no. 2, pp. 183-190.

Bijar, A.; Khayati, R. (2011): Segmentation of MS lesions using Active Contour Model, Adaptive Mixtures Method and MRF model. *2011 7th International Symposium on Image and Signal Processing and Analysis (ISPA)*, pp. 159-164.

Chalana, V.; Kim, Y. (1997): A methodology for evaluation of boundary detection algorithms on medical images. *IEEE Transactions on Medical Imaging*, vol. 16, no. 5, pp. 642-652.

Farag, A. A.; El-Baz, A. S.; Gimel'farb, G. (2006): Precise segmentation of multimodal images. *IEEE Transactions on Image Processing*, vol. 15, no. 4, pp. 952-968.

Greggio, N.; Bernardino, A.; Laschi, C.; Dario, P.; Santos-Victor, J. (2012): Fast estimation of Gaussian mixture models for image segmentation. *Machine Vision and Applications*, vol. 23, no. 4, pp. 773-789.

Gu, Y.; Kumar, V.; Hall, L. O.; Goldgof, D. B.; Li, C. Y. et al. (2013): Automated delineation of lung tumors from CT images using a single click ensemble segmentation approach. *Pattern Recognition*, vol. 46, no. 3, pp. 692-702.

Ji, Z.; Xia, Y.; Sun, Q.; Chen, Q.; Xia, D. et al. (2012): Fuzzy local Gaussian Mixture Model for brain MR image segmentation. *IEEE Transactions on Information Technology in Biomedicine*, vol. 16, no. 3, pp. 339-347.

Li-nan, F. L. F.; Dao-jing, L. D. L.; Shen-shen, S. S. S.; Chao-hai, C. C. C. (2010): Applied research on the automatic detection of lung nodules ROI based on Top-Hat and gabor filter. *Information Processing (ISIP), 2010 Third International Symposium on*, no. 1.

Lin, D. T.; Yan, C. R.; Chen, W. T. (2005): Autonomous detection of pulmonary nodules on CT images with a neural network-based fuzzy system. *Computerized Medical Imaging and Graphics*, vol. 29, no. 6, pp. 447-458.

Mansoor, A.; Bagci, U.; Xu, Z.; Foster, B.; Olivier, K. N. et al. (2014): Lung

Segmentation, vol. 33, no. 12, pp. 2293-2310.

Meng, L.; Zhao, H. (2009): A new lung segmentation algorithm for pathological CT images. *Proceedings of the 2009 International Joint Conference on Computational Sciences and Optimization, CSO 2009*, vol. 1, pp. 847-850.

Midthun, D. E. (2011): Screening for Lung Cancer. *Clinics in Chest Medicine*, vol. 32, no. 4, pp. 659-668.

Nguyen, T. M.; Wu, Q. M. J.; Member, S.; Ahuja, S. (2010): An extension of the standard mixture model for image segmentation. *IEEE Transactions on Neural Networks*, vol. 21, no. 8, pp. 1326-1338.

Sa, M. (2010): Image and video segmentation by combining unsupervised Generalized Gaussian Mixture Modeling and feature selection. *IEEE Transactions on Circuits and Systems for Video Technology*, vol. 20, no. 10, pp. 1373-1377.

Taha, A. A.; Hanbury, A. (2015): Metrics for evaluating 3D medical image segmentation: analysis, selection, and tool. *BMC Medical Imaging*, vol. 15, no. 1, pp. 29.

Wei, Q.; Hu, Y.; MacGregor, J. H.; Gelfand, G. (2008): Segmentation of lung lobes in clinical CT images. *International Journal of Computer Assisted Radiology and Surgery*, vol. 3, no. 5, pp. 151-163.

Yao, J.; Bliton, J.; Summers, R. M. (2013): Automatic segmentation and measurement of pleural effusions on CT, vol. 60, no. 7, pp. 1834-1840.

Zou, K. H.; Warfield, S. K.; Bharatha, A.; Tempany, C. M. C.; Kaus, M. R. et al. (2004): Statistical validation of image segmentation quality based on a spatial overlap index. *Academic Radiology*, vol. 11, no. 2, pp. 178-189.